Electronic Supplementary Information

Bioprocess development for muconic acid production from aromatic compounds and lignin

Davinia Salvachúa*, Christopher W. Johnson, Christine Singer, Holly Rohrer, Darren J. Peterson, Brenna A. Black, Anna Knapp, Gregg T. Beckham*

Materials and Methods

Strains and plasmid construction

Gene replacements in *Pseudomonas putida* KT2440 (ATCC 47054) were performed using previously described methods (See Johnson, C.W., Abraham, P.E., Linger, J.G., Khanna, P., Hettich, R.L., Beckham, G.T., 2017. Eliminating a global regulator of carbon catabolite repression enhances the conversion of aromatic lignin monomers to muconate in *Pseudomonas putida* KT2440. Metabolic Engineering Communications 5, 19–25). Briefly, plasmids containing gene expression cassettes, targeting regions, and markers for selection with kanamycin and counterselection with sucrose were constructed using Q5® Hot Start High-Fidelity 2X Master Mix (New England Biolabs) for amplifications and NEBuilder® HiFi DNA Assembly Master Mix (New England Biolabs) for assembly prior to transformation into NEB® 5-alpha F'I^q competent Escherichia coli (New England Biolabs). Plasmids were sequence verified by Sanger sequencing and transformed into *P. putida* by electroporation (see Choi, K.-H., Kumar, A., Schweizer, H.P., 2006. A 10-min method for preparation of highly electrocompetent Pseudomonas aeruginosa cells: Application for DNA fragment transfer between chromosomes and plasmid transformation. Journal of Microbiological Methods 64, 391–397). Integration of the non-replicative plasmids into the genome were selected on kanamycin and counterselection for the loss of the plasmid from the genome was performed using 25% sucrose. Gene replacements were identified by diagnostic colony PCR with MyTaq™ HS Red Mix (Bioline). Details on the construction of strains used in this study are included in Table S1, Table S2 contains plasmid construction details, and oligo sequences are listed in Table S3.

Tables

Table S1. Construction details for strains used in this study.

Strain	Genotype	Construction details
KT2440-CJ184	*P. putida* KT2440 Δ*catRBC*::Ptac:*catA* Δ*pcaHG*::Ptac:*aroY*:*ecdB*:*ecdD*	See Johnson, C.W., Salvachúa, D., Khanna, P., Smith, H., Peterson, D.J., Beckham, G.T., 2016. Enhancing muconic acid production from glucose and lignin-derived aromatic compounds via increased protocatechuate decarboxylase activity. Metabolic Engineering Communications 3, 111–119. doi:10.1016/j.meteno.2016.04.002
KT2440-CJ238	*P. putida* KT2440 Δ*catRBC*::Ptac:*catA* Δ*pcaHG*::Ptac:*aroY*:*ecdB*:*asbF* Δ*crc*	See Johnson, C.W., Abraham, P.E., Linger, J.G., Khanna, P., Hettich, R.L., Beckham, G.T., 2017. Eliminating a global regulator of carbon catabolite repression enhances the conversion of aromatic lignin monomers to muconate in *Pseudomonas putida* KT2440. Metabolic Engineering Communications 5, 19–25. doi:10.1016/j.meteno.2017.05.002
KT2440-CJ242	*P. putida* KT2440 Δ*catRBC*::Ptac:*catA* Δ*pcaHG*::Ptac:*aroY*:*ecdB*:*ecdD* Δ*crc*	*crc* was deleted from KT2440-CJ184 as for CJ238 in Johnson, C.W., Abraham, P.E., Linger, J.G., Khanna, P., Hettich, R.L., Beckham, G.T., 2017. Eliminating a global regulator of carbon catabolite repression enhances the conversion of aromatic lignin monomers to muconate in *Pseudomonas putida* KT2440. Metabolic Engineering Communications 5, 19–25. doi:10.1016/j.meteno.2017.05.002
KT2440-CJ475	*P. putida* KT2440 Δ*catRBC*::Ptac:*catA* Δ*pcaHG*::Ptac:*aroY*:*ecdB*:*ecdD* Δ*crc fpvA*:Ptac:*vanAB*	A Ptac:*vanAB* gene cassette was integrated in the intergenic region downstream of the gene *fpvA* (i.e. between *fpvA* (PP_4217) and PP_4218) in CJ242 using pCJ107. Plasmid integration at the locus downstream of *fpvA*, rather than in the *vanAB* locus, was diagnosed by amplification of a 1,496 bp product (3' junction) with primers oCJ550/oCJ312. Following sucrose selection, the integration of the gene cassette was confirmed by amplification of a 4254 bp product at the intergenic region downstream of *fpvA*, rather than the 2,081 wild-type product, using primers oCJ311/oCJ312.
KT2440-CJ518	*P. putida* KT2440 Δ*catRBC*::Ptac:*catA* Δ*pcaHG*::Ptac:*aroY*:*ecdB*:*ecdD* Δ*crc fpvA*:Ptac:*pobA*	A Ptac:*pobA* gene cassette was integrated in the intergenic region downstream of the gene *fpvA* in CJ242 using pCJ127. Plasmid integration at the *fpvA* locus, rather than in the *vanAB* locus, was diagnosed by amplification of a 1,132 bp product (3' junction) with primers oCJ633/oCJ312. Following sucrose selection, the integration of the gene cassette was confirmed by amplification of a 3,399 bp product at the intergenic region downstream of *fpvA*, rather than the 2,081 wild-type product, using primers oCJ311/oCJ312.

Table S2. Construction details for plasmids used for gene replacements in this study

Plasmid	Utility	Construction details
pCJ107	To integrate a second copy of *vanAB*, driven by the tac promoter and followed by the *tonB* terminator from *E. coli*, in the intergenic region downstream of the native terminator of *fpvA* in the genome of *P. putida* KT2440.	The upstream and downstream targeting regions for integration 3' of *fpvA* were amplified from *P. putida* KT2440 gDNA with primer pairs oCJ301/oCJ302 and oCJ306'/oCJ307, respectively. The *vanAB* cassette was amplified from P. putida KT2440 gDNA with oCJ369'/oCJ549', which incorporates the tac promoter. These products were then assembled into pK18mobsacB (ATCC 87097, Genbank accession FJ437239, see Schäfer, A., Tauch, A., Jäger, W., Kalinowski, J., Thierbach, G., Pühler, A., 1994. Small mobilizable multi-purpose cloning vectors derived from the *Escherichia coli* plasmids pK18 and pK19: selection of defined deletions in the chromosome of *Corynebacterium glutamicum*. Gene 145, 69–73.) amplified linearly with oCJ288 and oCJ289.
pCJ127	To integrate a second copy of *pobA*, driven by the tac promoter, in the intergenic region downstream of fpvA.	*pobA* was amplified from *P. putida* KT2440 genomic DNA with primer pair oCJ629/oCJ630 and assembled into pCJ107 digested with XbaI and SpeI to remove the *vanAB* genes.

Table S3. Primers used in this study

Primer	Sequence (5'-3'). Annealing portions are in bold type.	Description and annotation key
oCJ288	**CTAGCTTCACGCTGCCGCAAG**	pK18mobsacB linear forward
oCJ289	**CTAACTCACATTAATTGCGTTGCGCTCACTG**	pK18mobsacB linear reverse
oCJ301	AGTGAGCGCAACGCAATTAATGTGAGTTAG**AAGCCGAATGTCGATGATATCTACAACCTGAG**	Upstream targeting region 3' of *fpvA* forward with overlap for assembly with pK18mobsacB
oCJ302	GATTAATTGTCAACAGCTCGAATTC**AAAAAACCGCACCTGGGTGCG**	Upstream targeting region 3' of *fpvA* reverse and overlap for assembly with the EcoRI site and tac promoter
oCJ311	**AGCCTCTTCAGCGTCAAC**	Diagnostic: Outside of upstream targeting region forward
oCJ312	**CACGCCTGCTTCATTGAAC**	Diagnostic: Outside of downstream targeting region reverse
oCJ369'	TTTTTGAATTCGAGCTGTTGACAATTAATCATCGGCTCGTATAATGTGTGGAATTGTGAGCGGAT AACAATTTCACACTCTAGAGAGGAGGACAGCT**ATGTACCCCAAAAACACCTGGTACGTC**	*vanA* forward with tac promoter, EcoRI and XbaI sites, Shine-Delgarno consensus RBS, and overlap for assembly with upstream targeting region 3' of *fpvA*
oCJ549'	GCCTCCGGTCGGAGGCTTTTGACTACTAGTCTGAATGATATC**TCAGATGTCCAGCACCAGCAGC**	*vanB* reverse with SpeI and EcoRV sites and overlap for assembly with the tonB terminator
oCJ306'	ACTAGTAGTCAAAAGCCTCCGACCGGAGGCTTTTGACT**CATGGATGCCTGAAAGGCTCCCTTAC**	Downstream targeting region 3' of *fpvA* forward with tonB terminator and overlap for assembly with the *vanB* product
oCJ307	CCCTGAGTGCTTGCGGCAGCGTGAAGCTAG**GCCCCTCTGGAGAATCGAACGATG**	Downstream targeting region 3' of *fpvA* reverse with overlap for assembly with linear pK18mobsacB
oCJ550	TGCACCTGTATGTATGCG	Diagnostic: *vanB* forward
oCJ629	TGGAATTGTGAGCGGATAACAATTTCACACTCTAGAAAAGAAGGTAGTT**ATGAAAACTCAGGTTG CAATTATTGGTGCAGG**	*pobA* forward with an RBS designed using the Salis RBS calculator at https://salislab.net/software/ (see Salis, H.M., Mirsky, E.A., Voigt, C.A., 2009. Automated design of synthetic ribosome binding sites to control protein expression. Nat Biotechnol 27, 946–950.) and overlap for assembly with the XbaI site and tac promoter
oCJ630	TCAAAAGCCTCCGGTCGGAGGCTTTTGACTACTAGT**TCAGGCAACTTCCTCGAACGGC**	*pobA* reverse with overlap for assembly with the SpeI site and the tonB terminator
oCJ633	**CATTGCCGAGAACTATGTGG**	Diagnostic: *pobA* forward

Figures

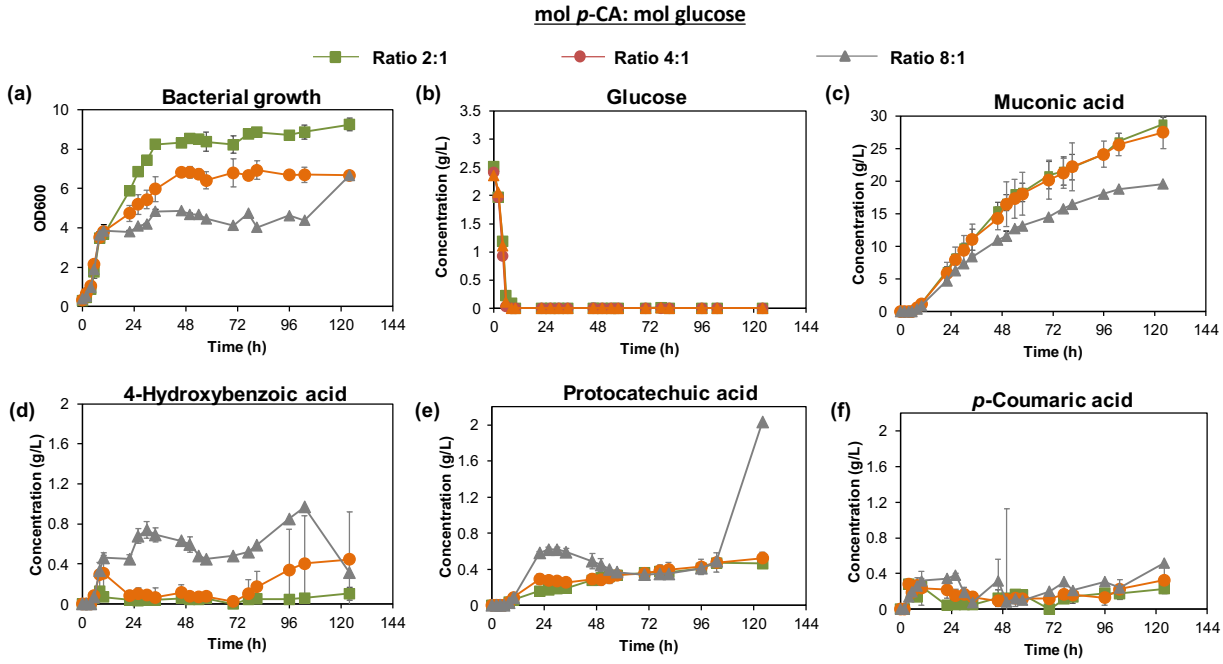

Fig. S1 MA production by *P. putida* KT2440-CJ184 in DO-stat fed-batch mode from three feeding solutions containing different *p*-CA (mol): glucose(mol) ratios (2:1, 4:1, and 8:1). Each value represents the average of biological duplicates. The error bars represent the absolute difference between the biological duplicates.

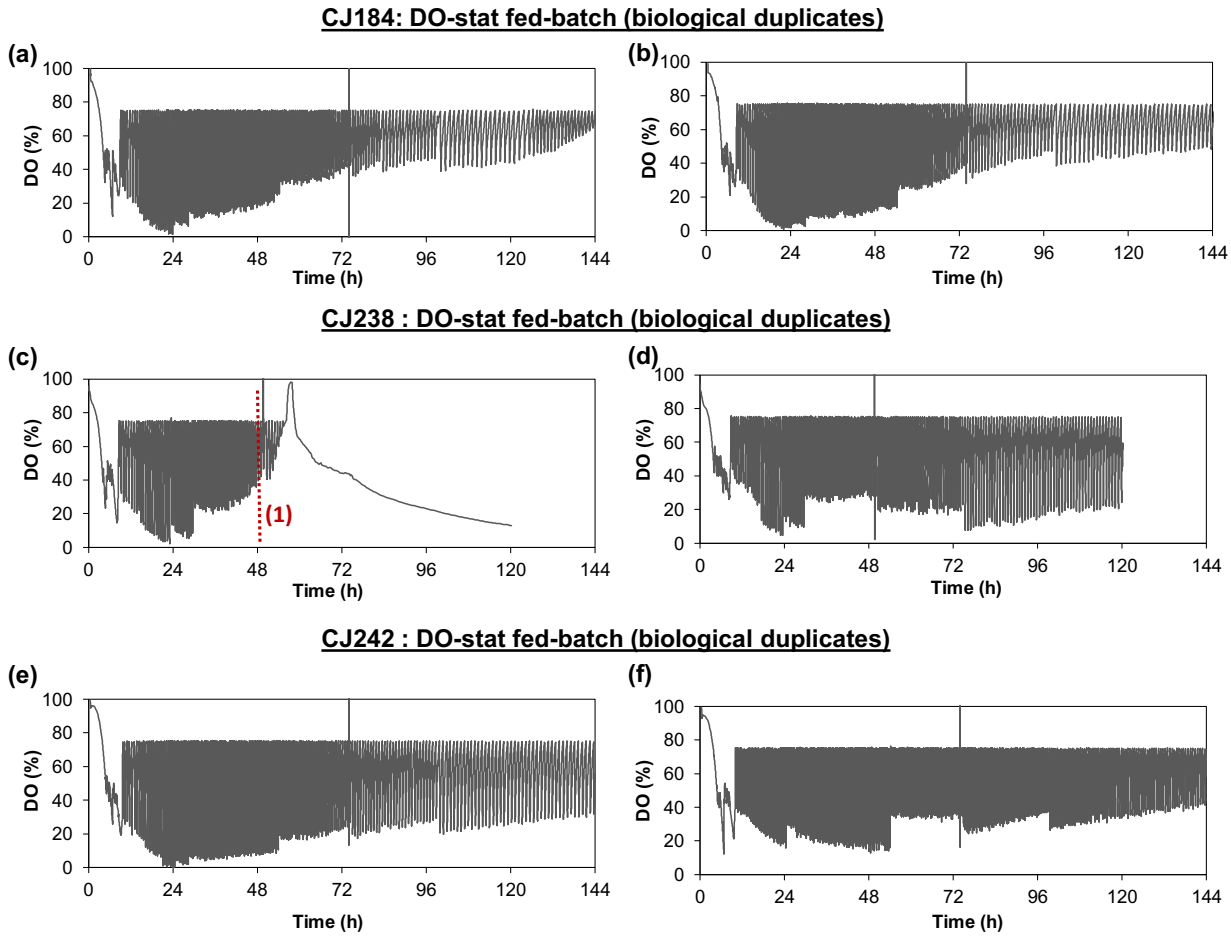

Fig. S2 Oxygen saturation (DO) profiles corresponding to the bioreactor experiments presented in Figure 2 a,b,c in the main manuscript. (1) Time at which the bacterium stopped utilizing glucose and could not be easily controlled by DO afterwards.

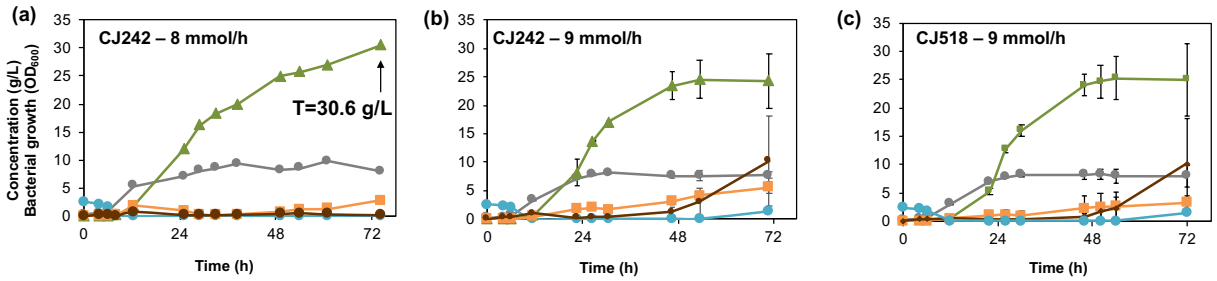

Fig. S3 MA production by *P. putida* KT2440-CJ242 and KT2440-CJ518 in constant fed-batch mode at two different feeding rates. (a) Single run with KT2440-CJ242 in which *p*-CA was fed at 8 mmol/h. (b) Results from a duplicated bioreactor run with KT2440-CJ242 in which *p*-CA was fed at 9 mmol/h. (c) Results from a duplicated bioreactor run with KT2440-CJ518 in which *p*-CA was fed at 9 mmol/h. *p*-CA concentration in the feeding bottle was 0.5 M at pH 7. The error bars represent the absolute difference between the biological duplicates.

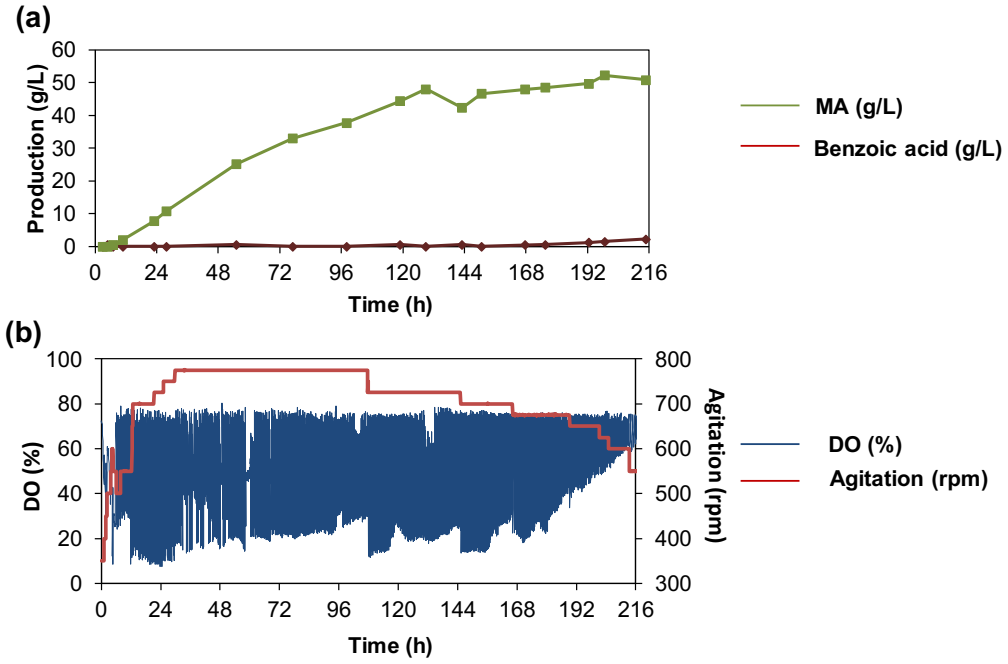

Fig. S4 MA production by *P. putida* KT2440-CJ242 in DO-stat fed-batch mode: (a) MA and benzoic acid concentration profiles. (b) DO (%) and agitation (rpm) profiles. Benzoic acid concentration in the feeding bottle was 160 g/L, glucose 100 g/L, and $(NH_4)_2SO_4$ 20 g/L at pH 7.

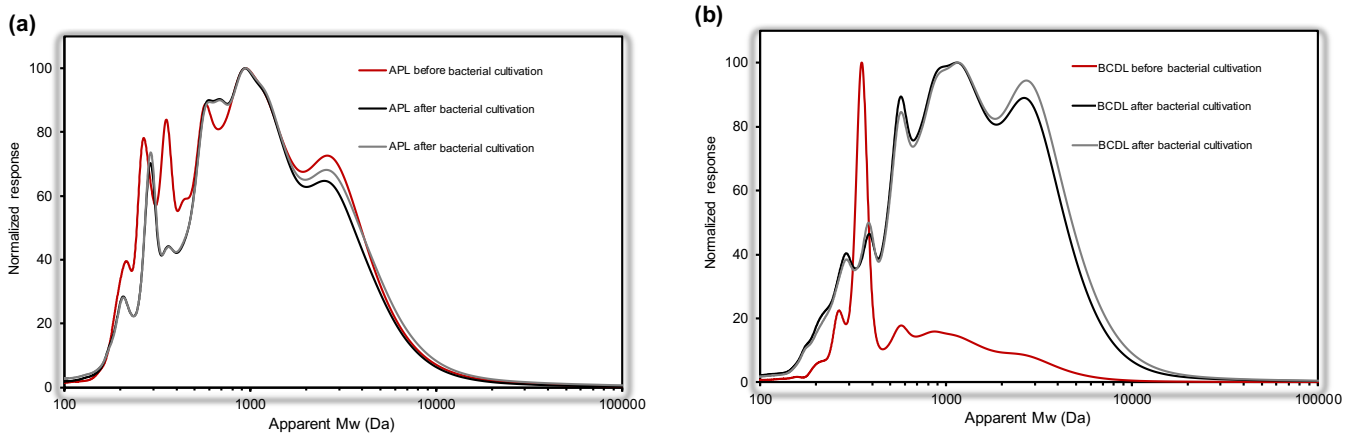

	Mp	Mn	Mw	PD
APL before bacterial cultivation	940	620	1800	2.9
APL after bacterial cultivation	940	660	1800	2.7
APL after bacterial cultivation	940	670	2200	3.3

	Mp	Mn	Mw	PD
BCDL before bacterial cultivation	350	760	1900	2.6
BCDL after bacterial cultivation	1100	800	2200	2.7
BCDL after bacterial cultivation	1200	620	1800	2.9

Fig. S5 Gel permeation chromatography profiles and data from the lignin in APL and BCDL before and after the bacterial cultivation with KT2440-CJ475 and KT2440-CJ242, respectively. The profiles from the duplicates after the bacterial cultivation are shown. Material and methods for sample preparation have been previously published in 'A. Rodriguez, D. Salvachúa, R. Katahira, B. A. Black, N. S. Cleveland, M. Reed, H. Smith, E. E. K. Baidoo, J. D. Keasling, B. A. Simmons, G. T. Beckham and J. M. Gladden, *ACS Sustainable Chemistry & Engineering*, 2017, **5**, 8171-8180'.

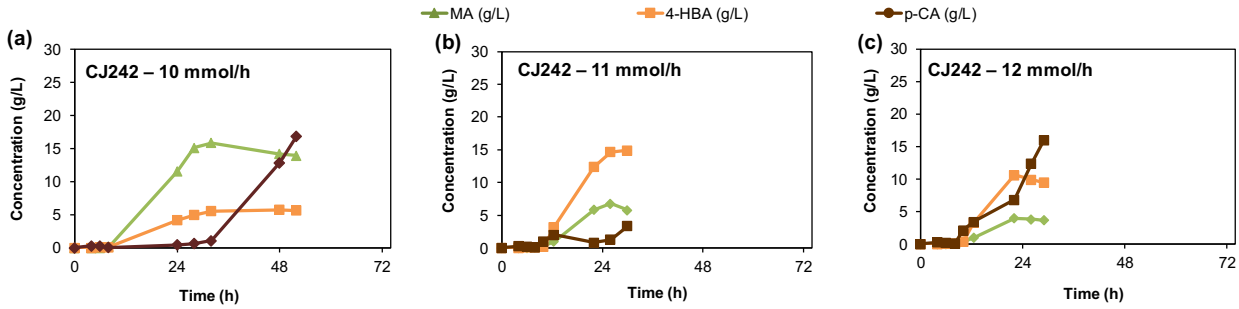

Fig. S6 MA production from *p*-CA by *P. putida* KT2440-CJ242 in constant fed-batch mode at different feeding rates: (a) 10 mmol *p*-CA/h, (b) 11 mmol *p*-CA/h, and (c) (b) 12 mmol *p*-CA/h. *p*-CA concentration in the feeding bottle was 0.5 M. This experiment was run in singlets.4-HBA= 4-hydroxybenzoic acid.